



# The use of active carbon pretreated at 2173 K as a support for palladium catalysts for hydrodechlorination reactions

Magdalena Bonarowska<sup>a</sup>, Wioletta Raróg-Pilecka<sup>b</sup>, Zbigniew Karpiński<sup>a,c,\*</sup>

<sup>a</sup> Institute of Physical Chemistry, Polish Academy of Sciences, ul. Kasprzaka 44/52, PL-01224 Warszawa, Poland

<sup>b</sup> Warsaw University of Technology, Faculty of Chemistry, ul. Noakowskiego 3, PL-00664 Warszawa, Poland

<sup>c</sup> Faculty of Mathematics and Natural Sciences-School of Science, Cardinal Stefan Wyszyński University, ul. Wóycickiego 1/3, PL-01938, Warszawa, Poland

## ARTICLE INFO

### Article history:

Received 3 August 2010

Received in revised form

10 December 2010

Accepted 13 December 2010

Available online 14 January 2011

### Keywords:

Turbostratic carbons

Carbon gasification

Pore structure

Carbon-supported Pd catalysts

CF<sub>2</sub>Cl<sub>2</sub>

Hydrodechlorination

## ABSTRACT

A commercial active carbon was heat-treated at 2173 K in argon and then subjected to steam gasification, yielding a series of very pure, turbostratic carbon materials, characterized by different specific surface areas and pore volume. These materials served as supports for palladium catalysts. Their pore structure, apparent absence of oxygen containing functional groups and hydrophobic character have a great effect on the dispersion of palladium introduced by impregnation. The use of an acetone solution of palladium acetate rather than an aqueous solution of palladium chloride (a typical Pd precursor) for the impregnation gives better results for preparing more metal dispersed Pd/C catalysts, especially for carbons with smaller micropore volumes. All preheated carbon-supported palladium catalysts showed very good activity and selectivity to CH<sub>2</sub>F<sub>2</sub> in CCl<sub>2</sub>F<sub>2</sub> (CFC-12) hydrodechlorination, up to 90% at the highest reaction temperature. In contrast, untreated or only HCl-washed carbons showed inferior catalytic properties. Residual phosphorus in the active carbons which were present in the active carbons which have not been subjected to thermal treatment, appears to be responsible for deterioration of catalytic properties of Pd/C. After reaction the presence of interstitial carbon (originating from the CFC-12 molecule) in the Pd lattice was found in the catalysts characterized by lower and medium metal dispersions.

© 2010 Elsevier B.V. All rights reserved.

## 1. Introduction

Besides of their primary application in adsorption processes, active carbons are commonly used as supports for catalytically active phases, such as metals or oxides. Catalytic hydrodechlorination (HdCl) of organic wastes is often realized with the use of carbon-supported Pt, Pd or Ni catalysts. Since this process is accompanied by massive release of HCl, active carbons, compared to typical oxidic carriers, are better suited to withstand highly corrosive reaction conditions, making them the support of industrial choice. Research with the use of such supports as silica or alumina, serves mainly for short-term model studies, when the functioning of various metallic (active) phases is tested. One important variable in the preparation of carbon supported hydrodechlorination catalysts is the selection and pretreatment of the support. In this respect, van de Sandt et al. found that purification of commercial active carbons by washing with aqueous NaOH, aqueous HCl and water resulted in an optimal performance of Pd/C hydrodechlori-

nation catalyst [1]. Apart from an exhaustive washing with acids and alkalis, a serious heat treatment of active carbons, at temperatures above 1773 K in inert gas, should also serve for effective purification of industrial active carbons [2,3]. Such pretreatment removes nearly all more or less volatile contaminants, especially typical catalytic poisons like S, As and P. This type of active carbon has already found application as a support of modified ruthenium catalyst used in ammonia synthesis [4]. Its relatively low specific surface area and less developed pore structure (compared to thermally untreated carbons) may be improved by subsequent gasification using steam or carbon dioxide [2,5,6], making the support very useful for various applications. It was our hope that the highly pretreated active carbon should also serve as a useful support for metal-containing catalysts in hydrodechlorination of various harmful compounds, such as CCl<sub>4</sub>. Deprived of a vast majority of functional (e.g. oxygen-carrying) groups, a strongly hydrophobic nature of highly pretreated carbons would help in more effective adsorption of CCl<sub>4</sub> from wastewaters. Subsequent hydrodechlorination on metal (usually Pt or Pd) sites located in the porous structure of carbon should efficiently transform this harmful molecule into more benign products.

This paper describes the results on preparation and characterization of palladium catalysts supported on differently pretreated samples of Norit GF40 carbon, the support which has been recently

\* Corresponding author at: Institute of Physical Chemistry, Polish Academy of Sciences, Department of Catalysis on Metals, ul. Kasprzaka 44/52, PL-01224 Warszawa, Poland. Tel.: +48 22 3433356; fax: +48 22 3433333.

E-mail address: [zkarpinski@ichf.edu.pl](mailto:zkarpinski@ichf.edu.pl) (Z. Karpiński).

**Table 1**  
Characteristics of differently pretreated samples of Norit GF40 carbon.

Carbon designation	Pretreatment code <sup>a</sup>	Mass loss after gasification, wt%	Ash, wt%	Density, g/cm <sup>3</sup>
A	GF40/H <sub>2</sub> O	–	0.52	0.29
B	GF40/HCl	–	0.26	0.29
C	GF40/HCl/2173	–	0.16	0.4
D	GF40/HCl/2173/1033	1.1	0.17	0.39
E	GF40/HCl/2173/1103	11.24	0.21	0.34
F	GF40/HCl/2173/1120	20.37	0.30	0.3
G	GF40/HCl/2173/1129	28.93	0.36	0.26
H	GF40/HCl/2173/1158	51.3	0.55	0.24

<sup>a</sup> For details see Section 2. H<sub>2</sub>O and HCl stand for washing media, “2173” means the temperature (in K) of GF40 pretreatment in argon, and the last figure (for example: 1120) is the temperature of steam gasification.

employed in catalytic studies [7]. In addition, the hydrodechlorination behavior of these catalysts was tested in H<sub>2</sub>Cl of dichlorodifluoromethane, the reaction selected as a relatively simple one, frequently investigated in the past decade on differently supported palladium catalysts, also on carbon-supported Pd [1,8–12]. Therefore, it was convenient to compare the catalytic performance of Pd supported on thermally treated carbon with previously investigated Pd/support catalysts.

## 2. Experimental

A series of different active carbons were prepared on the basis of Norit GF 40, the starting material obtained from the Norit B.V. Company. The first sample, called A, was obtained by washing the parent carbon with large portions of redistilled water (to remove the dusty fraction). Another sample (B) was obtained after washing with hydrochloric acid (analar). The rest of GF 40 was subjected to a high-temperature heating at 2173 K for 2 h, in argon atmosphere, yielding a larger batch of sample C. Because such a procedure led to a considerable carbon graphitization and drastic decrease of specific surface area (*vide infra*), subsequent gasification of sample C with a steam:Ar = 1:1 mixture at temperatures between 1033 and 1158 K for 5 h, led to preparation of next active carbon samples characterized by a gradually higher degree of burn-off (samples D, E, F, G and H). Table 1 collects the sample pretreatment and a preliminary characteristics of obtained carbon materials.

Surface areas and porosities were measured with an ASAP 2020 instrument from Micromeritics, employing the BET (Brunauer–Emmett–Teller), t-Plot, BJH (Barrett–Joyner–Halenda) and HK (Horvath–Kawazoe) methods and using nitrogen as adsorbate. Before measuring the adsorption isotherm at 77 K, the activated carbon was kept at 473 K for 5 h in vacuum to clean its surface. Possible presence of selected elements in starting, washed and preheated GF40 carbon was done by the X-ray fluorescence method. XRF analyses were done with the use of a Philips PW 2400 spectrometer at the Institute of Geology in Warsaw, Poland. Presence of sulfur in selected active carbon samples was excluded by the Schöniger method of analysis at the Institute of Organic Chemistry of PAS in Warsaw. Table 2 shows the analytical results.

**Table 2**  
Results of analysis of activated carbons subjected to different pretreatments.

Carbon sample (pretreatment code <sup>a</sup> )	P, wt%	Cl, wt%	Mg, wt%	Fe, wt%	Ca, wt%	S, wt%
Untreated GF40	0.186	0.018	0.008	0.006	0.026	– <sup>b</sup>
A (GF40/H <sub>2</sub> O)	0.137	– <sup>b</sup>	– <sup>b</sup>	0.005	0.015	– <sup>b</sup>
B (GF40/HCl)	0.103	0.147	– <sup>b</sup>	0.004	0.008	– <sup>b</sup>
C (GF40/HCl/2173)	0.011	– <sup>b</sup>	– <sup>b</sup>	0.002	0.016	– <sup>b</sup>

<sup>a</sup> For sample pretreatment code see Table 1 and text.

<sup>b</sup> Not found.

Two series of palladium/carbon catalysts were prepared by the incipient wetness impregnation of crushed and sieved carbons (grain fraction 0.6–1.25 mm), using an aqueous solution of palladium chloride (analytical purity, POCh Gliwice, Poland), slightly acidified with HCl (analar), or acetone (analytical purity) solution of palladium acetate (spectral purity from Ventron, Karlsruhe, Germany). After impregnation the materials were dried overnight at 373 K. Then they were reduced in a fluidized reactor in an H<sub>2</sub>/Ar flow. During reduction the temperature was increased at a rate 8 K/min from RT to 673 K and kept at 673 K for 3 h. After reduction the catalysts were flushed with argon and transferred in air to glass-stoppered bottles, which were stored in a dessicator.

The respective catalyst code includes both the type of carbon support (as in Table 1) and the kind of Pd precursor, for example, Pd(Cl)/C denotes the catalyst prepared by deposition of PdCl<sub>2</sub> on carbon C, whereas Pd(Ac)/G stands for the catalyst prepared from Pd acetate on carbon G. The palladium loading was 2 wt%.

The Pd/C catalysts were characterized by CO chemisorption (at 308 K, using a backsorption method with an ASAP 2020 Chem instrument from Micromeritics), temperature programmed (palladium) hydride decomposition (TPHD, for details, see [13]), and X-ray diffraction (XRD, Siemens D5000, Ni-filtered Cu K $\alpha$  radiation).

Temperature-programmed desorption (TPD) of the decomposition products of surface oxygen groups was performed for a few representative samples of GF40: B, C, G and one catalyst, Pd(Ac)/G. The TPD experiments were carried out in a flow reactor coupled to a Dycor Ametek MA200 quadrupole mass spectrometer, in the manner previously described [14]. A tested sample (mass ~0.45 g) was placed in the reactor and heated to 1100 K at a 10 K/min ramp in a flow of helium (25 cm<sup>3</sup>/min), while selected mass signals were observed at 15 s intervals. The obtained mass spectra allowed to represent evolution of CO<sub>2</sub> and CO, the main products of decomposition of the-surface oxygen-containing groups.

Prior to reaction (and also prior to CO chemisorption and TPD), all catalysts (all samples ~0.2 g) were reduced in flowing 10% H<sub>2</sub>/Ar (25 cm<sup>3</sup>/min), raising the temperature from room temperature to 623 K (at 8 K/min), and kept at 623 K for 2 h. The reaction of dichlorodifluoromethane (CFC-12 from Galco S.A., Belgium; purity 99.9%) with hydrogen (purified over MnO/SiO<sub>2</sub>) was conducted in a glass flow system under atmospheric pressure at 433, 443 and 453 K, in the manner previously described [8,15]. Briefly, feed partial pressures were 15 and 150 Torr (1 Torr = 133.3 N m<sup>-2</sup>) of dichlorodifluoromethane and hydrogen, respectively, in an argon carrier and the overall flow rate of the reactant gas mixture was 100 cm<sup>3</sup>/min. The reaction mixture leaving the reactor was analyzed by GC. In order to adequately establish changes in the catalytic behavior, a typical reaction run lasted ~24 h. The first stage of the reaction involved a 20-h period at 453 K, when the catalyst performance was stabilized. Next, the reaction temperature was lowered, in 10 K steps, and the next experimental points were collected. After catalyst screening at the lowest reaction temperature (433 K) the catalyst performance was tested again at 453 K, giving, in most cases, a good return to the initial behavior at this temperature. To avoid secondary reactions, the overall conversion was usually kept

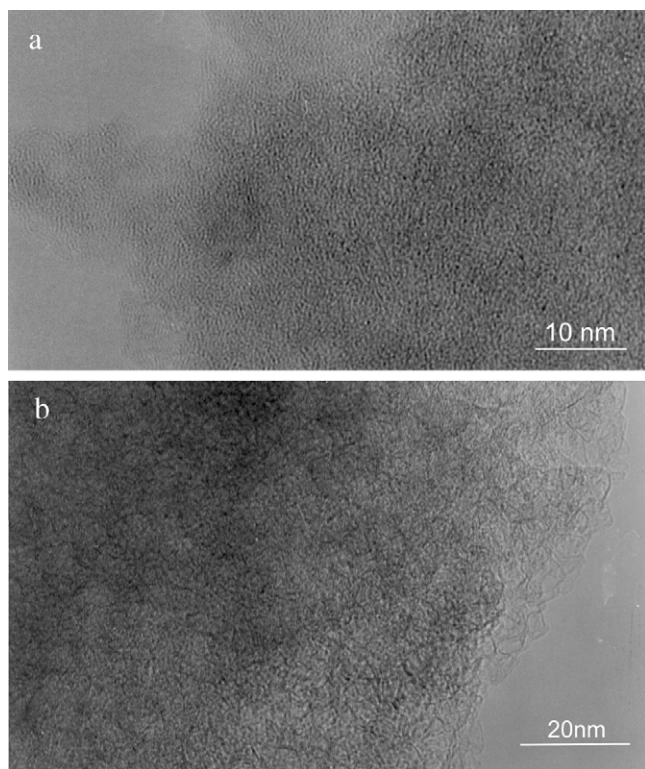


**Fig. 1.** TEM images of Norit GF40: (a) starting GF40, (b) GF40 pretreated at 2173 K (carbon C).

low, i.e. <10%, at the highest reaction temperature. Post-reaction catalytic samples were also investigated by XRD.

### 3. Results and discussion

#### 3.1. Turbostratic carbons

Fig. 1 shows two TEM images showing the morphology of the starting GF40 carbon and that of the preheated carbon at 2173 K. The morphology change caused by the preheating is well recognized: in a completely amorphous structure starting carbon (Fig. 1a) it is possible to recognize the presence of parallel graphene layers (Fig. 1b).

The X-ray diffraction patterns for the differently pretreated Norit GF40 carbon samples are shown in Fig. 2. The diffractograms of thermally untreated GF40 samples (A and B) indicate their amorphous character. The only characteristic feature is a diffuse peak corresponding to the (002) reflection at  $\sim 22.2^\circ$ . On the other hand, all thermally treated carbons (irrespective of their further gasification) showed turbostratic two dimensional ordering. First, a much better developed (002) peak was shifted upwards to  $\sim 24.2^\circ$ . Next, the (100) and (101) reflections merge into a single (10) peak, at  $\sim 43.5^\circ$ . Similarly, the (11) peak is manifested at  $\sim 79^\circ$ . It is seen that even very pronounced gasification (>50%) of highly heated carbon (sample H) which results in an almost complete recovery of specific surface area (Table 3), does not lead to loss of turbostratic character of gasified samples. In addition, a small but very sharp peaks at  $\sim 26.4^\circ$  (characteristic for graphite) are well seen on the right side of the (002) reflections of turbostratic carbons. So, in line with TEM, XRD confirms a partial ordering of the carbon.

Fig. 3 shows nitrogen adsorption–desorption isotherms on differently pretreated Norit GF40 active carbons. Carbons A and B (B is not shown in Fig. 3) exhibit a type I isotherm of nitrogen at 77 K (according to Brunauer), indicating a large number of micropores.

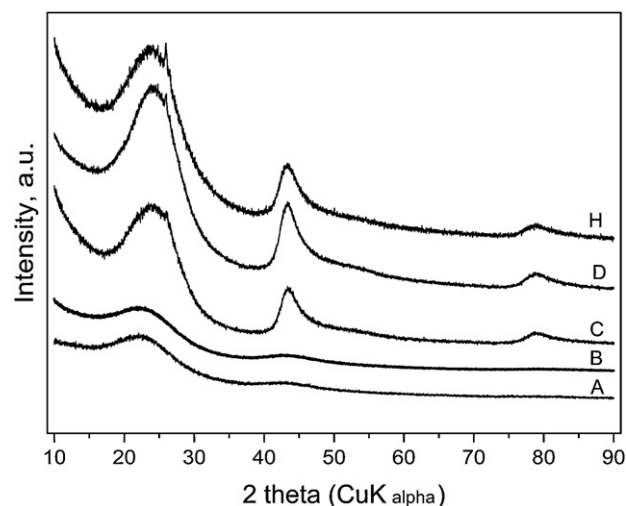


**Fig. 2.** XRD profiles of differently pretreated Norit GF40 samples.

Carbon C (after annealing at 2173 K) shows very small specific surface area ( $26 \text{ m}^2/\text{g}$ ). A gradually increased degree of gasification with steam results in a vast recovery of the specific surface area and porous structure (Table 3).

Upon 51.3% mass burn-off, the specific surface area of carbon H ( $1794 \text{ m}^2/\text{g}$ ) matches that exhibited by carbons A ( $1885 \text{ m}^2/\text{g}$ ) and B ( $1676 \text{ m}^2/\text{g}$ ). However, the shape of  $\text{N}_2$  adsorption isotherms of “gasified” carbons loses a “langmuirian” shape, with a regular increase of hysteresis loop, indicating the presence of mesopores. Fig. 4 shows the evolution of porous structure with the degree of gasification of the thermally pretreated GF40. Clearly, both micro- and mesopores develop upon carbon burn-off.

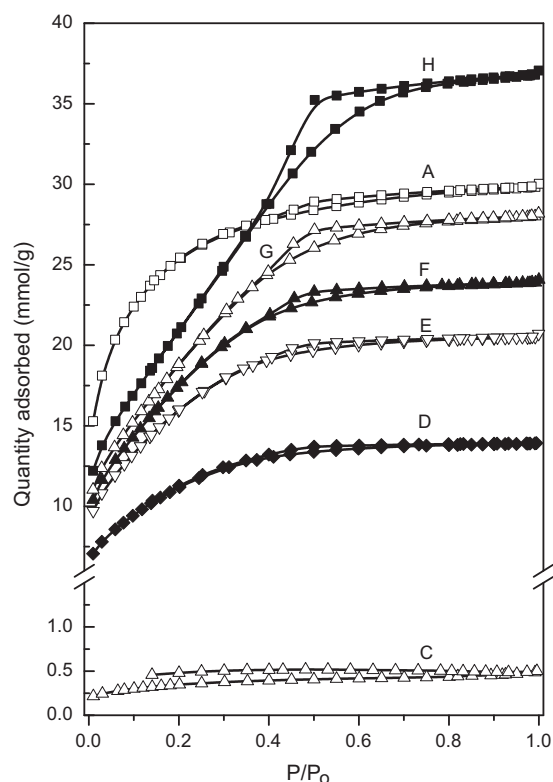


**Fig. 3.** Adsorption–desorption isotherms of  $\text{N}_2$  (at 77 K) on differently pretreated Norit GF40 active carbons.

**Table 3**  
Characteristics of untreated and pretreated Norit GF40 active carbon samples.

Carbon designation	Pretreatment code <sup>a</sup>	$S_{\text{BET}}$ , m <sup>2</sup> /g	t-Plot micropore area, m <sup>2</sup> /g	t-Plot external surface area, m <sup>2</sup> /g	Pore volume, <sup>b</sup> cm <sup>3</sup> /g	DFT pore volume, cm <sup>3</sup> /g	
						Total	Pores <0.5 nm
A	GF40/H <sub>2</sub> O	1885	— <sup>c</sup>	— <sup>c</sup>	1.03	0.889	0.430
B	GF40/HCl	1676	1583	93	0.953	0.814	0.074
C	GF40/HCl/2173	26.5	10.4	16.1	0.0036	0.0024	0
D	GF40/HCl/2173/1033	848	815	34	0.481	0.408	0
E	GF40/HCl/2173/1103	1256	1192	64	0.710	0.622	0
F	GF40/HCl/2173/1120	1423	1315	107	0.825	0.725	0
G	GF40/HCl/2173/1129	1526	1319	207	0.970	0.861	0
H	GF40/HCl/2173/1158	1794	1333	461	1.278	1.141	0

<sup>a</sup> For sample pretreatment code see Table 1.

<sup>b</sup> HK (Horvath–Kawazoe) method.

<sup>c</sup> Not measured.

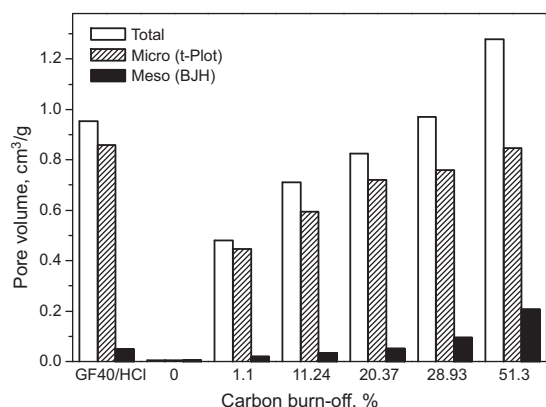


**Fig. 4.** Development of pore structure by steam gasification of highly pretreated Norit GF40 active carbon.

Temperature-programmed desorption from representative samples of GF40 and one Pd/C catalyst is shown in Fig. 5a (CO<sub>2</sub> evolution) and Fig. 5b (CO evolution). It is seen that sample B of GF40 (without preheating at 2173 K, washed in HCl and pretreated in Ar at 773 K) exhibits very pronounced profiles of CO<sub>2</sub> and CO lib-

eration. However, samples C and G show only negligible evolution of carbon oxides, indicating a very small presence of oxygen functionalities on these materials. A similar situation is with a reduced Pd(Ac)/G catalyst, where a small peak in CO<sub>2</sub> profile, at 700–900 K, would result from a residual presence of acetate precursor.

In conclusion, the gradually steam-gasified GF40 samples regain the considerable surface area and porous structure lost in the high temperature pretreatment of this Norit active carbon. Interestingly enough, they also acquire a substantial degree of mesoporosity.

### 3.2. Carbon-supported palladium catalysts

Deposition of palladium precursors on variously pretreated Norit GF40 carbon produced different results, was found strongly dependent on the type impregnating medium and degree of carbon burn-off produced by steam gasification. Assessment of homogeneity of Pd particle size comes from the XRD study of freshly reduced (and post-reaction) Pd/C samples (Fig. 6), and indirectly from TPHD (temperature programmed hydride decomposition, Fig. 7) investigation, the method which was applied earlier for such diagnostic purposes [8].

XRD examination established that some catalysts were composed of larger Pd crystallites (~20 nm in size) and a part of a

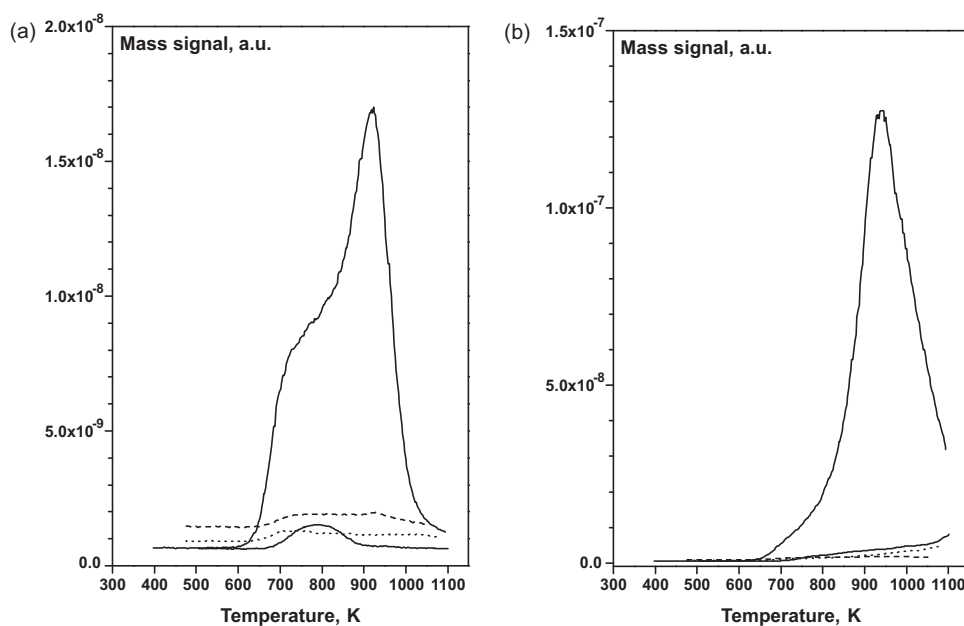


**Fig. 5.** Temperature-programmed desorption profiles of selected samples of GF40 and Pd(Ac)/G catalyst. (a) CO<sub>2</sub> evolution, (b) CO evolution. Carbon B—thick line, carbon C—dotted line, carbon G—dashed line, Pd(Ac)/C—thin solid line.



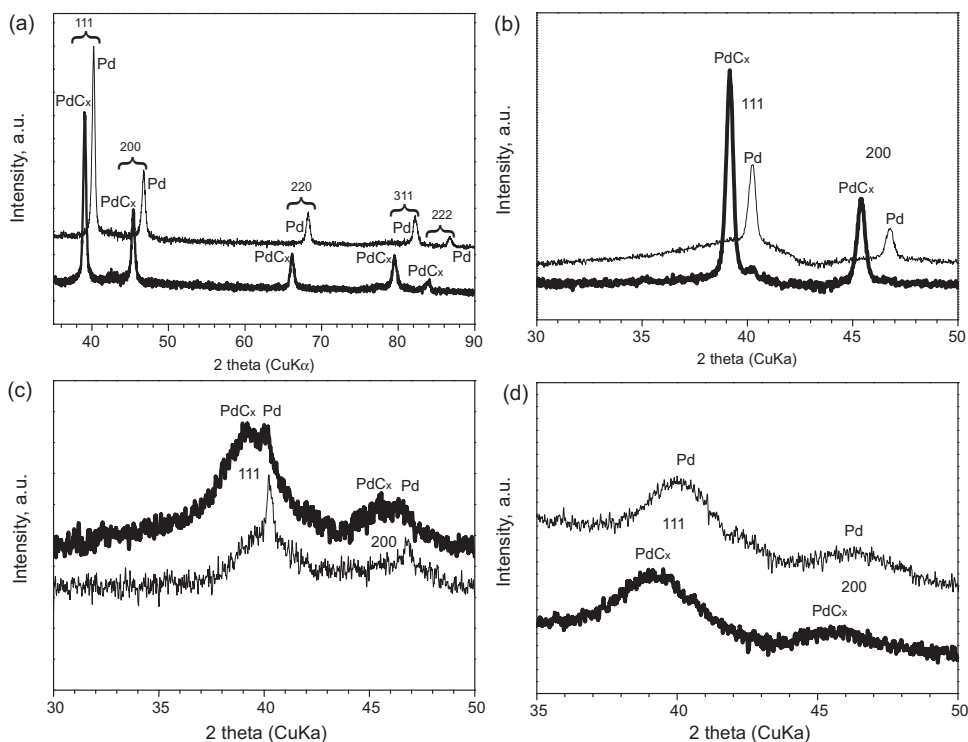


**Fig. 6.** XRD of selected Pd/C catalysts: (a) Pd(Ac)/C, (b) Pd(Cl)/D, (c) Pd(Cl)/F and (d) Pd(Cl)/F. Thin lines—reduced samples, thick lines—post-reaction samples. The presence of basic reflections from fcc phase of Pd and Pd–C solid solution (PdC<sub>x</sub>) are marked.

more dispersed Pd material, as concluded from an overlapping of a very sharp (1 1 1) diffraction peak and a diffuse (1 1 1) Pd reflection (Fig. 6c). In other cases (exemplified in Fig. 6a, b and d), the obtained reflections were found practically not structured, suggesting the presence of palladium characterized by a narrower distribution of metal crystallites.

In the case of the TPHD method, which uses the phenomenon of a facile  $\beta$ -PdH formation at a relatively low hydrogen pressure, a narrow, single TPHD peak implies the  $\beta$ -PdH decomposition from similar in size palladium particles, whereas double/multiple and structured in shape TPHD peaks suggest the presence of palladium phase characterized by a broader distribution of particle size [8]. In addition, a shift of peak minimum towards lower temperatures indicates the presence of smaller Pd particles [8]. Such low temperature TPHD minima are also less intense, because the H/Pd ratio in bulk Pd hydride decreases when Pd particle size decreases [10],

so it is difficult to confirm the presence of a  $\beta$ -PdH phase in highly dispersed Pd material (like for Pd(Cl)/H in Fig. 7). In other cases the TPHD profiles presented in Fig. 6 exhibit various situations described above. Results of a more careful analysis of TPHD and XRD profiles are shown in Table 4, yielding important information on the degree of homogeneity of Pd materials.

Table 4 collects the experimental data from CO chemisorption, TPHD and XRD. It is seen that the use of acetone solution of Pd acetate gives more homogeneous Pd catalysts than when aqueous solution of PdCl<sub>2</sub> was used for preparation. In the case of the latter precursor, for carbons D, E, F and G, the palladium material is present as small particles as well as larger crystallites. Only in the case of the carbon H which was the most intensively gasified, the kind of Pd precursor does not appear to have effect on metal dispersion.

Table 4 also shows that for Pd/A and Pd/B catalysts there is a serious conflict between the Pd dispersion data assessed from CO chemisorption and XRD. A considerable metal dispersion (FE) concluded from the absence of characteristic palladium reflections, being a sign of a considerable metal high dispersion (FE), is not reflected in the CO uptake. This is presumably because the surface of palladium supported on not preheated carbons A and B contains considerable amounts of phosphorus (Table 2), which as a typical catalytic poison hampered the CO uptake. This fact is also reflected in the catalytic behavior of these catalysts (*vide infra*). For the rest of Pd/C catalysts, the agreement between XRD and CO chemisorption data is fair or good (Table 4), especially if one accepts known problems with a partial blocking of palladium surface by carbon species originating from the support [17].

Similar results were obtained in preparation of Pd catalysts supported on turbostratic carbons, pretreated at 1223 K [17]. Fairly narrow Pd particle size distributions were obtained for the catalysts made by impregnation of a THF solution of palladium acetylacetonate. In contrast, broader distributions were obtained when an aqueous solution of PdCl<sub>2</sub> was used: large Pd particles up to 45 nm were observed. Although those authors [17] related this fact to

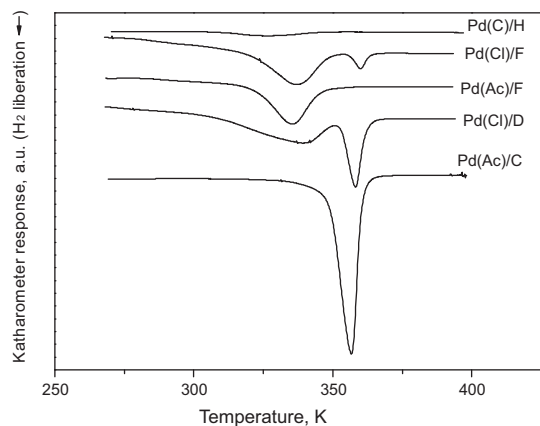


**Fig. 7.** Temperature-programmed hydride decomposition profiles of selected Pd/C catalysts.

**Table 4**  
Characteristics of Pd/C catalysts.

Catalyst designation <sup>a</sup>	Fraction exposed (FE = CO/Pd)	Pd particle size, nm			Results of TPHD	
		From CO/Pd <sup>b</sup>	Crystallite size from XRD <sup>c</sup> after reduction	Crystallite size from XRD <sup>c</sup> after reaction	H/Pd from hydride decomposition	Temperature of minimum in TPHD, K
Pd(Cl)/A	0.0077	146	<2 <sup>d</sup>	<2 <sup>d</sup>		No PdH decomposition
Pd(Ac)/A	0.0187	60	<2 <sup>d</sup>	<2 <sup>d</sup>		No PdH decomposition
Pd(Cl)/B	0.0285	39.3	<2 <sup>d</sup>	<2 <sup>d</sup>		No PdH decomposition
Pd(Ac)/B	0.0714	15.7	<2 <sup>d</sup>	<2 <sup>d</sup>		No PdH decomposition
Pd(Cl)/C	0.0173	64.6	32.6	22.2 (PdC <sub>x</sub> ) + 24.9 (Pd)	0.50	361.5
Pd(Ac)/C	0.0149	75.1	20.2	19.2 (PdC <sub>x</sub> )	0.46	357.1
Pd(Cl)/D	0.137	8.2	10 + 22.5	21.1 (PdC <sub>x</sub> ) + 22.3 (Pd)	0.35	339.8, 358.5
					(0.22 + 0.13) <sup>e</sup>	
Pd(Ac)/D	0.054	20.7	22.3	21 (PdC <sub>x</sub> )	0.36	358.1
Pd(Cl)/E	0.124	9.0	5.1 + 23.0	3.9	0.27	333.8, 357.7
				(PdC <sub>x</sub> ) + 23.4(PdC <sub>x</sub> ) + 23.5(Pd)	(0.20 + 0.07) <sup>e</sup>	
Pd(Ac)/E	0.199	5.6	4.2	3.6 (PdC <sub>x</sub> )	0.16	328.5
Pd(Cl)/F	0.138	8.1	4.7 + 20.5	4.8 (PdC <sub>x</sub> ) + 19.2 (Pd)	0.24	337.7, 360.7
					(0.22 + 0.02) <sup>e</sup>	
Pd(Ac)/F	0.149	7.5	3.9	4.2 (PdC <sub>x</sub> )	0.21	336.4
Pd(Cl)/G	0.185	6.1	5.0	4.2 (PdC <sub>x</sub> )	0.21(0.18 + 0.03) <sup>e</sup>	330, 353.4
Pd(Ac)/G	0.228	4.9	3.9	4.6 (PdC <sub>x</sub> )	0.18	332.7
Pd(Cl)/H	0.236	4.7	4.1	6.3 (PdC <sub>x</sub> )	0.04	327.2
Pd(Ac)/H	0.225	5.0	4.4	3.6 (PdC <sub>x</sub> )	0.16	335.6

<sup>a</sup> For further details see Section 2 and Table 3.

<sup>b</sup> Calculated as  $d = 1.12/\text{FE}$ , according to [16].

<sup>c</sup> From the broadening of (1 1 1) reflections (using the Scherrer equation). Crystallite sizes from the most abundant phases are underlined (PdC<sub>x</sub>—carbon solution in palladium).

<sup>d</sup> Extremely diffuse, practically invisible XRD reflections from Pd.

<sup>e</sup> For two minima in TPHD profiles (last column), a H/Pd contribution from each hydrogen liberation is accordingly marked in the brackets.

problems associated with catalyst passivation (coalescence of non-passivated Pd particles upon exposure to air), we believe that in our case the use of an organic medium (less polar than water) is beneficial for distributing the Pd precursor in a pore structure of a hydrophobic carbon material, mostly deprived of oxygen-containing functional groups. Such a situation takes place when the pore structure of original GF40 Norit carbon is not fully recovered after carbon pretreatment (2173 K + gasification), i.e. for samples D, E, F and G. Carbon H, characterized by much larger surface area and pore volume (Table 2), is able to accommodate larger amounts of smaller clusters of Pd precursors more uniformly, irrespective of their chemical nature and impregnating medium. Therefore, possible problems associated with a wettability of hydrophobic support [18] are important only when its porous structure is not sufficiently developed.

Similarly, Ehrburger et al. [19] found a direct correlation between the degree of dispersion of platinum supported on a graphitized carbon black and the extent of prior gasification (in air) of the carbon support. Interestingly, the degree of dispersion of platinum for the catalyst impregnated with aqueous solution of H<sub>2</sub>PtCl<sub>6</sub> was found to be 24% compared to 55% obtained for the same catalyst loading when impregnation was carried out in a benzene–ethanol mixture. The authors [19] assumed that a more uniform distribution of chloroplatinic acid (from a benzene–ethanol solution) on the substrate should give a higher degree of metal dispersion. Then, they consider that the dielectric constant of the benzene–ethanol solution mixture is much less than that of water, so chloroplatinic acid is present essentially as undissociated molecules in the former medium, whereas in the aqueous solution it is strongly ionized, platinum being present in the anionic form, [PtCl<sub>6</sub>]<sup>2−</sup>. In conclusion, the mentioned authors believe that chloroplatinic acid should be adsorbed nonspecifically, molecularly and uniformly from a benzene–ethanol mixture. Carbons which are poor adsorbents for anions, are able to adsorb chloroplatinic acid from an aqueous solution as agglomerates in the form of islands or clusters giving rise to a broad distribution of particle sizes. Our

results with an aqueous solution of anionic Pd precursor (PdCl<sub>2</sub> in HCl is supposed to turn H<sub>2</sub>PdCl<sub>4</sub>) and acetone solution of neutral Pd(CH<sub>3</sub>COO)<sub>2</sub> do not confirm the suggestion mentioned above. As long as the porous structure is well developed (i.e. for carbon samples G and H) the differences in metal dispersion are not large. Similar results were obtained by Gurrath et al. [20] who used different Pd precursors (anionic, neutral and cationic) introduced to carbons characterized by considerable surface areas and pore volumes. In this respect, one refers to an earlier report of Rodriguez-Reinoso et al. [21] on characterization of Fe/C catalysts prepared from aqueous solutions of iron nitrate and n-pentane solutions of iron pentacarbonyl. The carboxylic groups of the activated carbon supports were crucial to facilitate the access of the aqueous solution to the small pores, whereas this was not the case for nonpolar pentane solvent.

### 3.3. Catalytic behavior of Pd/C in dichlorodifluoromethane hydrodechlorination

Fig. 8a exemplifies the procedure of catalyst testing described in Section 2. It is seen that after catalyst's "passivation" at 453 K, further changes in the reaction temperature (down to 443 and 433 K) produce stable conversions (and product selectivities) in very short periods of time and a final "return" to the initial reaction temperature (453 K) brings back the previous catalytic behavior. Catalytic screening of all Pd/C samples prepared with use of highly pretreated active carbons showed that stable conversions are achieved in a relatively short "passivation" time (<2 h). This is demonstrated in Fig. 8a and b, where also product selectivities are shown to be quickly established at a constant level. Methane, difluoromethane (HFC-32), and, to a much smaller extent, chlorodifluoromethane (HCFC-22) were found to be the predominant products. For Pd samples supported on highly pretreated carbons the first two compounds make up usually more than 97% of all products. The remaining products (mainly CHClF<sub>2</sub> and C<sub>2</sub>H<sub>6</sub>, CClF<sub>3</sub>, CHF<sub>3</sub>, and CH<sub>3</sub>Cl) make up <4% of all products at 453 K.

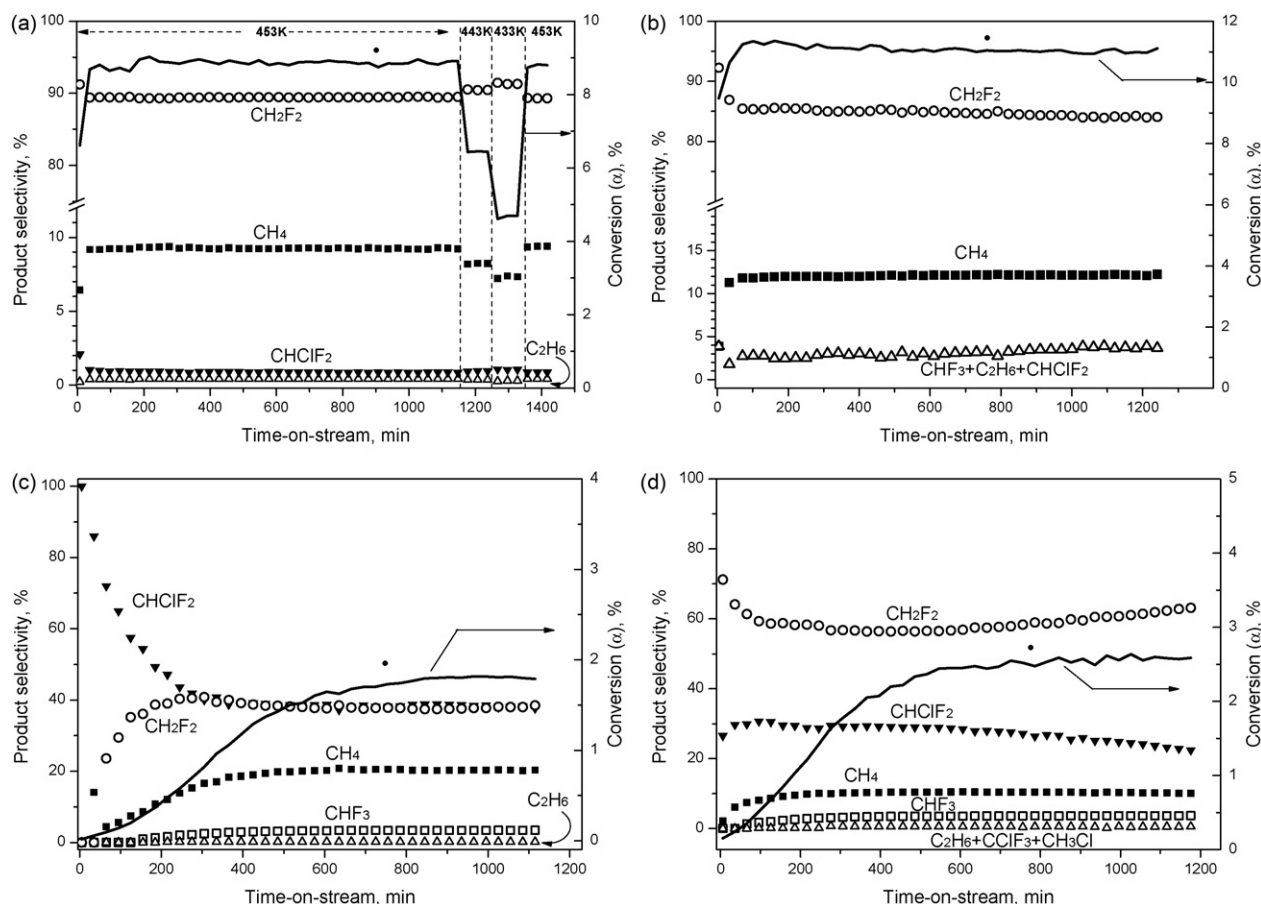


**Fig. 8.** Time-on-stream behavior in  $\text{CCl}_2\text{F}_2$  hydrodechlorination on selected samples of Pd/C catalysts at 453 K: (a) Pd(Cl)/F, where also the screening procedure is shown (catalyst stabilization at 453 K, then the decrease of reaction temperature to 443 K and 433 K, and return to 453 K, see Section 2), (b) Pd(Ac)/H, (c) Pd(Ac)/A, and (d) Pd(Ac)/B.

Noticeable exceptions are Pd/C samples based on non-preheated activated carbons (A and B), for which larger changes in overall conversions and in product selectivities are expanded over longer time intervals (Fig. 8c and d). As it was mentioned in Section 2 (Table 2), carbon B (washed with HCl), and especially carbon A (washed with distilled water) contain nonnegligible amounts of phosphorus (GF40 is chemically activated using  $\text{H}_3\text{PO}_4$ ). Partial removal of phosphorus by HCl wash slightly improves the catalytic behavior: both the conversion level as well as the selectivity towards  $\text{CH}_2\text{F}_2$  are increased for Pd(Ac)/B. Further improvement of the catalytic behavior of Pd(Ac)/A and Pd(Ac)/B observed with time-on-stream must also result from additional decontamination during hydrodechlorination (due to HCl and HF evolution) at 453 K. Because our main attention was focused on the behavior of thermally treated carbon-supported catalysts, further work with the catalysts supported on carbons A and B was suspended.

The results of catalytic tests at steady state are presented in Table 5. The turnover frequency, as a measure of catalytic activity, was calculated by using metal dispersion data assessed from XRD of used catalysts (FE in the first column of Table 5). With very few exceptions, the selectivities to  $\text{CH}_2\text{F}_2$  (desired reaction product) were measured at overall conversions <10%, so they should result from initial product distributions. It is seen that, apart from catalysts supported on carbons A and B, the selectivities to  $\text{CH}_2\text{F}_2$  are very high, usually between 80 and 90%, for the highest reaction temperature. The trend in the activation energy (higher  $E_A$ 's for carbons A and B, last column in Table 5) also reflects the need of removing contaminants from active sites (here phosphorus). In general, the level of  $E_A$ 's (52–62 kJ/mol) is similar to that obtained for carbon-supported palladium catalysts in earlier reports [9,10].

The selectivity level of ~90% obtained in this study is characteristic for the best previously investigated Pd/C catalysts [1,8–12,15]. A similar conclusion concerns the overall activity (TOF) of the most active catalysts tested in this study [9,15,22,23].

Fig. 9 shows the correlation between the turnover frequency and palladium dispersion for thermally treated carbon Pd catalysts. Contaminated carbons (A and B) are excluded from this relation. It is seen that among 12 tested Pd/C catalysts, 11 of them show a

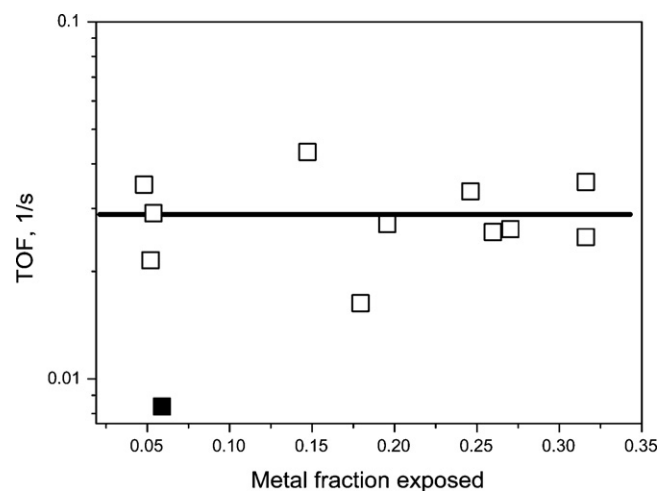


**Fig. 9.** TOF as a function of metal dispersion in  $\text{CCl}_2\text{F}_2$  hydrodechlorination on Pd/C catalysts. Black square represents the behavior of Pd(Ac)/C catalysts (average from three runs).

**Table 5**  
Kinetic data for 1.5 wt% Pd/C: turnover frequencies and selectivities towards CH<sub>2</sub>F<sub>2</sub> at three reaction temperatures (433, 443 and 453 K), and apparent activation energies (*E<sub>A</sub>*'s).

Catalyst <sup>a</sup> (FE <sup>b</sup> )	TOF, s <sup>-1</sup> (S <sub>CH<sub>2</sub>F<sub>2</sub></sub> , %)			<i>E<sub>A</sub></i> , kJ/mol
	433 K	443 K	453 K	
Pd(Cl)/A (0.75 <sup>c</sup> )	0.000769 (53.8%)	0.00113 (52.1%)	0.00157e–3 (51.0%)	61.9 ± 1.1
Pd(Ac)/A (0.75 <sup>c</sup> )	0.000787 (43.1%)	0.00124 (40.3%)	0.0017 (38.0%)	62.8 ± 1.0
Pd(Cl)/B (0.75 <sup>c</sup> )	0.00105 (69.5%)	0.00168 (68.0%)	0.00245 (63.0%)	58.4 ± 3.4
Pd(Ac)/B (0.75 <sup>c</sup> )	0.000852 (69.3%)	0.0012 (66.0%)	0.00178 (65.6%)	62.5 ± 1.7
Pd(Cl)/C (0.048)	0.0152 (85.1%)	0.0227 (83.2%)	0.0324 (81.7%)	57.9 ± 0.9
Pd(Ac)/C (0.059)	0.00434 (83.2%)	0.00662 (81.3%)	0.00837 (80.8%)	55.7 ± 1.0
Pd(Cl)/D (0.054)	0.0151 (85.6%)	0.0202 (84.0%)	0.0291 (88.1%)	55.1 ± 2.0
Pd(Ac)/D (0.052)	0.0112 (90.7%)	0.0157 (89.3%)	0.0215 (82.4%)	53.3 ± 3.0
Pd(Cl)/E (0.196)	0.0141 (87.9%)	0.0209 (86.5%)	0.0272 (85.2%)	55.5 ± 1.4
Pd(Ac)/E (0.316)	0.0186 (88.8%)	0.0259 (87.3%)	0.0356 (86.0%)	52.5 ± 0.1
Pd(Cl)/F (0.147)	0.0227 (91.4%)	0.0313 (90.5%)	0.0432 (89.5%)	53.7 ± 0.5
Pd(Ac)/F (0.260)	0.0134 (90.7%)	0.0187 (89.7%)	0.0258 (88.5%)	53.0 ± 0.3
Pd(Cl)/G (0.270)	0.0132 (90.8%)	0.0188 (89.7%)	0.0263 (88.4%)	54.5 ± 0.8
Pd(Ac)/G (0.246)	0.0168 (92.2%)	0.0246 (91.3%)	0.0335 (90.4%)	53.8 ± 0.6
Pd(Cl)/H (0.179)	0.00808 (75.0%)	0.0114 (72.3%)	0.0158 (70.5%)	56.1 ± 0.9
Pd(Ac)/H (0.316)	0.013 (87.3%)	0.0188 (85.4%)	0.025 (84.0%)	53.6 ± 1.7

<sup>a</sup> As in Table 4.

<sup>b</sup> Calculated as FE = 1.12/d, according to [16], where d is the metal crystallite measured by XRD after reaction (see Table 4).

<sup>c</sup> Approximate FE values assuming that Pd particle size is 1.5 nm in (very diffuse XRD lines).

similar level of catalytic activity (open squares in Fig. 9). Such a result seems to be in apparent disagreement with our earlier data obtained for Pd/Al<sub>2</sub>O<sub>3</sub> catalysts, where a mild (i.e. with TOF changes within an order of magnitude over the complete FE range) correlation between TOF and metal dispersion was found [15]. Although a more clear-cut explanation of this difference is not offered here, we should admit that our present results encompass only a limited range of palladium dispersion (FE between 0.05 and 0.30). On the other hand, the black square in Fig. 8, which deviates from the suggested correlation (thick line), shows the average behavior assessed from three independent runs with the Pd(Ac)/C catalyst.

The fact that >90% of tested catalysts showed a direct correlation in confrontation with only a single “unfitting” catalyst suggested to leave this problem behind. Our lack of enthusiasm in this matter was also associated with the fact that carbon C is the sample which was thermally treated, but it was not subjected to gasification. So, its surface area was very low and pore structure very limited, making this sample not very attractive as a catalyst support. We would also suspect that such a drastic thermal treatment would yield very inhomogeneous carbon material and, in effect, non-uniform distribution of deposited palladium material.

Fig. 6 showing the XRD profiles of Pd/C catalysts demonstrates the presence of Pd–C solution in the samples subjected to CCl<sub>2</sub>F<sub>2</sub> hydrodechlorination. Carbiding of palladium-containing catalysts in CCl<sub>2</sub>F<sub>2</sub> hydrodechlorination is a well-known phenomenon. It is manifested in a substantial retention of carbon (originating from CCl<sub>2</sub>F<sub>2</sub> molecule) in the palladium lattice, as the presence of palladium–carbon solutions (up to a PdC<sub>0.13</sub>) has been ascertained using XRD [8,11,15,24–29]. By analogy with the formation of β-palladium hydride, a more effective carbon incorporation to Pd is expected for larger Pd particles [30]. In line with such an interpretation, McCauley [30] and Morato et al. [27] found less carbon in Pd catalysts characterized by smaller crystallite sizes. Fig. 6c and, especially, d shows that bulk carbiding of smaller Pd crystallites (catalysts Pd(Cl)/F and Pd(Ac)/F with the Pd crystallite size less than 5 nm) proceeds during reaction. It appears that during CCl<sub>2</sub>F<sub>2</sub> hydrodechlorination, massive amounts of bare C<sub>1</sub> species (after the removal of all halogens) become very effective carbiding agents. Fig. 8a and b shows that the selectivity to methane slightly increases at the initial stage of reaction. This effect could be due to a gradually less effective removal of C<sub>1</sub> species via their incorporation to

Pd bulk. Slowing down this process creates a better possibility for hydrogenating these species to methane.

#### 4. Conclusions

Highly preheated (at 2173 K) commercial active carbon, subjected to steam gasification at different temperatures, yielded a series of very pure, turbostratic carbon materials, characterized by different specific surface areas and pore volumes. Gasification of highly sintered active carbons with steam gradually restores the surface area and pore structure of the starting carbon. These materials served as supports for palladium catalysts tested in CCl<sub>2</sub>F<sub>2</sub> hydrodechlorination. The pore structure and hydrophobic character of highly preheated carbons have a great effect on dispersion of palladium precursor introduced by impregnation. Impregnation with acetone solution of palladium acetate brings better results than using an aqueous solution of palladium dichloride, especially for carbons with smaller micropore volumes. It seems that a limited wettability with water of carbons deprived of functional groups (in effect of high temperature treatment) results in deposition of larger clusters of Pd precursors and, in effect, leads to preparation of low metal dispersed catalysts, and inhomogeneous particle size distribution. All highly preheated carbon-supported palladium catalysts showed very good activity and selectivity in hydrodechlorination of dichlorodifluoromethane (selectivity to CH<sub>2</sub>F<sub>2</sub> up to 90%). In contrast, untreated and or only HCl-washed carbons showed much poorer catalytic properties. Residual phosphorus, present in the active carbons which have not been subjected to thermal treatment, appears to be responsible for deterioration of catalytic properties of Pd/C. Catalytic performance of these catalysts is markedly improved during reaction, suggesting that the phosphorus content is decreasing due to interaction with HCl and HF, products liberated during hydrodehalogenation.

After reaction the presence of interstitial carbon (originating from the CFC-12 molecule) in the Pd lattice was found in the catalysts characterized by lower and medium metal dispersions.

#### Acknowledgements

This work was supported by the Polish Ministry of Science and Higher Education within Research Project No. N N204 161636. We



are also grateful to Norit B.V. Company for providing us with commercially manufactured activated carbon materials.

## References

- [1] E.J.A.X. van de Sandt, A. Wiersma, M. Makkee, H. van Bekkum, J.A. Moulijn, *Appl. Catal. A* 173 (1998) 161–173.
- [2] L. Forni, D. Molinari, I. Rossetti, N. Pernicone, *Appl. Catal. A* 185 (1999) 269–275.
- [3] X. Zheng, S. Zhang, J. Xu, K. Wei, *Carbon* 40 (2002) 2597–2603.
- [4] R.B. Strait, *Nitrogen Methanol* 238 (1999) 37–43.
- [5] Z. Kowalczyk, S. Jodzis, W. Raróg, J. Zieliński, J. Pielaszek, A. Presz, *Appl. Catal. A* 184 (1999) 95–102.
- [6] Z. Kowalczyk, J. Sentek, S. Jodzis, R. Diduszko, A. Presz, A. Tetrzyk, Z. Kucharski, J. Suwalski, *Carbon* 34 (1996) 403–409.
- [7] R.F. Bueres, E. Asedegbega-Nieto, E. Díaz, S. Ordóñez, F.V. Díez, *Catal. Today* 150 (2010) 16–21.
- [8] M. Bonarowska, J. Pielaszek, V.A. Semikolenov, Z. Karpiński, *J. Catal.* 209 (2002) 528–538.
- [9] B. Coq, F. Figuéras, S. Hub, D. Tournigant, *J. Phys. Chem.* 99 (1995) 11159–11166.
- [10] B. Coq, J.M. Cognion, F. Figuéras, D. Tournigant, *J. Catal.* 141 (1993) 21–33.
- [11] A. Malinowski, W. Juszczak, J. Pielaszek, M. Bonarowska, M. Wojciechowska, Z. Karpiński, *Stud. Surf. Sci. Catal.* 130 (2000) 1991–1996.
- [12] M. Bonarowska, B. Burda, W. Juszczak, J. Pielaszek, Z. Kowalczyk, Z. Karpiński, *Appl. Catal. B* 35 (2001) 13–21.
- [13] M. Bonarowska, Z. Karpiński, *Polish J. Chem.* 82 (2008) 1973–1979.
- [14] G.S. Szymański, Z. Karpiński, S. Biniak, A. Świątkowski, *Carbon* 40 (2002) 2627–2639.
- [15] W. Juszczak, A. Malinowski, Z. Karpiński, *Appl. Catal. A* 166 (1998) 311–319.
- [16] S. Ichikawa, H. Poppa, M. Boudart, *J. Catal.* 91 (1985) 1–10.
- [17] N. Krishnakutty, M.A. Vannice, *J. Catal.* 155 (1995) 312–326.
- [18] L. Daza, S. Mendioroz, J.A. Pajares, *Carbon* 24 (1986) 33–41.
- [19] P. Ehrburger, O.P. Mahajan, P.L. Walker Jr., *J. Catal.* 43 (1976) 61–67.
- [20] M. Gurrath, T. Kuretzky, H.P. Boehm, L.B. Okhlopov, A.S. Lisitsyn, V.A. Likholobov, *Carbon* 38 (2000) 1241–1255.
- [21] F. Rodríguez-Reinoso, C. Salina-Martínez de Lecea, A. Sepúlveda-Escribano, J.D. López-González, *Catal. Today* 7 (1990) 287–298.
- [22] A.L. Dantas Ramos, P. da Silva Alves, D.A.G. Aranda, M. Schmal, *Appl. Catal. A* 277 (2004) 71–81.
- [23] Y.C. Cao, Y. Li, *Appl. Catal. A* 294 (2005) 298–305.
- [24] E.J.A.X. van de Sandt, A. Wiersma, M. Makkee, H. van Bekkum, J.A. Moulijn, *Catal. Today* 35 (1997) 163–170.
- [25] E.J.A.X. van de Sandt, A. Wiersma, M. Makkee, H. van Bekkum, J.A. Moulijn, *Appl. Catal. A* 155 (1997) 59–73.
- [26] M. Öcal, M. Maciejewski, A. Baiker, *Appl. Catal. B* 21 (1999) 279–289.
- [27] A. Morato, C. Alonso, F. Medina, Y. Cesteros, P. Salagre, J.E. Sueiras, D. Tichit, B. Coq, *Appl. Catal. B* 32 (2001) 167–179.
- [28] M. Bonarowska, A. Malinowski, W. Juszczak, Z. Karpiński, *Appl. Catal. B* 30 (2001) 187–193.
- [29] A. Malinowski, W. Juszczak, M. Bonarowska, J. Pielaszek, Z. Karpiński, *J. Catal.* 177 (1998) 153–163.
- [30] J.A. McCaulley, *J. Phys. Chem.* 97 (1993) 10372–10379.